Korean J. Chem. Eng., **25**(4), 721-726 (2008)

Biomass gasification in internal circulating fluidized beds: a thermodynamic predictive tool

Francesco Miccio*,,†, Karel Svoboda*,***, Jean-Pierre Schosger*, and David Baxter***

*European Commission, Joint Research Center, Institute for Energy JRC/IE, P.O. Box 2 1755 ZG Petten, The Netherlands
**Istituto di Ricerche sulla Combustione, Consiglio Nazionale delle Ricerche, Napoli, Italy
***Institute of Chemical Process Fundamentals, Academy of Sciences, Praha, Czech Republic
(*Received 13 December 2006 • accepted 5 October 2007*)

Abstract−The paper deals with a high efficiency process for biomass gasification based on the concept of the internal circulating fluidized bed (ICFB). A modeling tool has been developed for the prediction of theoretical values for the main species in a syngas produced by ICFB gasification. A thermodynamic sub-model has been utilized and integrated with a simplified lumped model of the gasifier. The model predicts H_2 concentration up to 61% on water free basis. The comparison with calculations for one stage gasification demonstrates ICFB process is preferable, no dilution with inert gas occurring. Among the studied variables, the steam/fuel ratio and the fuel moisture exert the largest influence on the hydrogen yield with percentage changes up to 15% in the explored range of the variables.

Key words: Gasification, Biomass, Fluidized Bed, Hydrogen, Thermodynamics

INTRODUCTION

The use of renewable fuels in high efficiency processes is strongly promoted worldwide and particularly in Europe as a consequence of the application of the Kyoto protocol on CO_2 reduction, European Union legislation targets, and the rising oil and natural gas prices. Among the objectives of the European Union policy, the effective use of biomass and wastes, particularly biodegradable wastes, as fuel sources, for power generation, for transport, or storage as an alternative fuel has a high priority [1]. The gasification of biomass or waste produces a syngas consisting of a mixture of carbon dioxide, carbon monoxide, methane and hydrogen. It can be directly used for powering internal or external combustion engines for electricity generation in the range 0.1-10 MW_{el} [2]. Furthermore, biomass gasification is greatly appealing for hydrogen generation and hot fuel cell application, where waste heat can be used for the endothermic gasification process [3]. So far, a hydrogen-rich syngas with very low nitrogen content is beneficial for the process efficiency, since heat losses are minimized.

Atmospheric fluidized bed gasification is a viable and flexible technology for biomass and wastes, since different fuels can be processed even with large differences in chemical and physical properties, including biomass, municipal wastes, industrial residuals, and food wastes [4-6]. Nevertheless, relevant issues have still to be addressed, namely purification of the syngas with regard to tar and particulate matter, the achievement of a high conversion rate and gas heating value, the maximization of hydrogen content, the conversion of poorly reactive char [7-9].

The Internal Circulating Fluidized Bed (ICFB) concept has been successfully applied for biomass gasification [10,11]. The major advantage of this option is the possibility of carrying out the process in two separate but interconnected chambers, where different operating conditions can be set. The two vessels are normally operated under reducing, meaning gasification, and oxidizing, meaning combustion, atmospheres, respectively. Thus, two distinct gas streams are generated: the flue gas exiting the oxidizing/combustion chamber and the syngas exiting the reducing/gasification chamber. The heat transferred from the former to the latter chamber enhances the endothermic fuel conversion in the reducing zone. The main advantage is the production of syngas with potentially high heating value and rich in combustible species, since dilution with nitrogen is avoided. Furthermore, in the combustion zone, where an excess air condition is maintained, the conversion of char particles readily occurs, limiting carbon comminution and elutriation that is huge in single-stage atmospheric FB gasification [9,12].

The general objective of the research deals with the production of alternative fuels from biomass and waste, with particular focus on hydrogen. The present paper reports on a modeling tool for the prediction of limit values for the main components of a syngas produced by ICFB gasification. The study focuses on a biomass fuel to be processed in a gasification rig on laboratory scale. A thermodynamic sub-model has been used and integrated with a simplified lumped model of the gasifier. Thus, this study is preparatory for an experimental activity on biomass gasification in the course of development at JRC/IE. The outcomes of the modeling activity are reported and discussed in the paper.

MODEL DESCRIPTION

A mathematical model of the fluidized bed gasifier has been developed to estimate the syngas composition under thermodynamic equilibrium conditions for an ICFB gasifier [13]. Fig. 1A shows the concept of the ICFB gasifier, with two distinct vessels arranged concentrically in the test equipment. The fluidized bed reactor (left/outer side) accomplishes the gasification reactions, whereas the riser (right/inner side) is the place where the combustion occurs. The process is assumed at steady state and under adiabatic conditions. Steam

†To whom correspondence should be addressed.
E-mail: miccio@irc.cnr.it

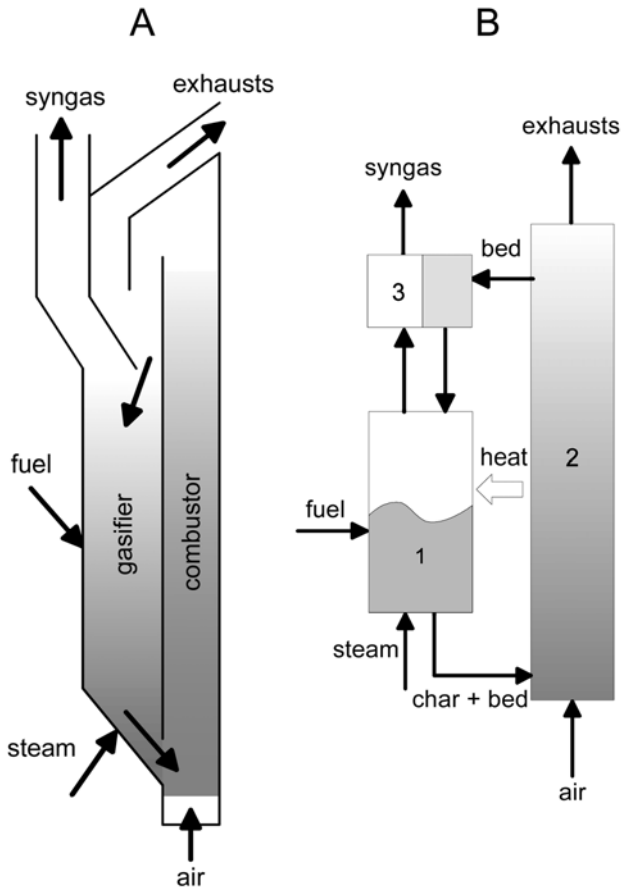

Fig. 1. Concept of the internal circulating fluidized bed with the two zones of gasification and combustion (A) and its lumped model schematization (B).

as gasifying medium and preheated air for the partial fuel combustion in the riser are considered. The bed circulation between the two vessels allows for the heat transfer from the combustion chamber to the gasification zone. Char particles are entrained with the bed, burnt in the riser, and may be circulated several times before full conversion. The ICFB has been modeled as a combination of two continuous stirred tank reactors (see Fig. 1B), the first one for the fuel pyrolysis and gasification, the second one for the char combustion. Block 3 represents the separator of gaseous and solid streams; this block does not contribute to chemical reactions. The two reactors 1 and 2 exchange mass and energy as indicated in Fig. 1B. Total char combustion is assumed, and thermodynamic equilibrium is imposed for the gasifier.

The Computer Program for Calculation of Complex Chemical Equilibrium Compositions and Applications (CEA) of NASA [14] has been used for thermodynamic calculations. It has been integrated in an MS Excel worksheet for computing the heat and mass balances in the whole system with an iterative procedure. The CEA routine calculates the system temperature, the thermodynamic properties, and the molar fraction of the chemical species present at equilibrium, when the mass flow rate, temperature and formation enthalpy of each species entering the reactor are assigned. For the biomass under consideration, the chemical formula $C_2H_{3.71}O_{1.82}N_{0.02}$ has been adopted, according to the ultimate fuel analysis of Table 1. In turn, the chemical formula of volatiles is $C_2H_{6.3}O_{3.09}N_{0.03}$, as obtained from a stoichiometric balance based on both proximate and ultimate analyses on dry basis. The molar formation enthalpy of the volatiles is required as an input parameter for the CEA routine. It has been calculated on the basis of the assumed composition of the volatiles as the difference between the combustion enthalpy of one mole of volatiles and the combustion enthalpy of total C and H contained in its molecule. Further assumptions are:

(i) The fuel fed into reactor 1 forms a char and a volatile stream upon drying and pyrolysis.

(ii) The char conversion in reactor 1 is negligible, whereas the char is completely burnt in the combustor/riser 2 where it is circulated together with the sand.

(iii) The volatiles are converted by steam in reactor 1.

(iv) Heat transfer occurs between the two reactors by wall conduction and by the convection mechanism that is associated with the bed circulation.

(v) The circulation rate for the bed material is a function of the bed inventory and the riser fluidization velocity.

It is worth noting that the assumption ii) is justified by the increased char reactivity during combustion, up to 3-4 orders of magnitude higher than during gasification [15], as well as by the rather similar residence times of char particles in the gasification and combustion zones at high circulation rate.

The solution for the gasifier (reactor 1) is straightforward, once all input variables are assigned to the CEA routine. Only the volatiles are considered for CEA calculations, the char not being converted in the gasifier. Other species entering reactor 1 are the water (moisture in the biomass) and the steam, the gasification medium. The mass flow rate of the char entering the riser (reactor 2) is calculated based on the fuel proximate analysis.

Since the endothermic step associated with devolatilization occurs in the gasifier, the heat needed for pyrolysis also has to be taken into account [16]. The heat exchanged between reactor 1 and riser 2 must be considered as an additional input for the CEA program, because it affects the enthalpy of the reactants. This enthalpy difference ΔH is the sum of the heat transferred by both convection and conduction (Eq. (1)).

$$\Delta H = W_b \gamma_b (T_1 - T_2) + S\Lambda (T_1 - T_2) \quad (1)$$

The energy balance for the riser 2 reads:

$$W_{ch}\gamma_{ch}(T_1 - T_{ref}) + W_a\gamma_a(T_a - T_{ref}) - W_{ex}\gamma_{ex}(T_2 - T_{ref}) + W_{ch}\Theta_{ch} + \Delta H = 0 \quad (2)$$

The symbols W, γ, Λ, and Θ are used for flow rate, specific heat, coefficient of heat transfer, and fuel heating value. S is the internal surface between reactor 1 and 2. The subscripts b, ch, a, and ex mean bed, char, air, and exhausts, respectively.

The bed circulation rate W_b is calculated via Eq. (3), where a linear dependence on the square root of the fluidized bed height h and on the slip velocity $U_2 - U_t$ is assumed, U_2 is the fluidization velocity in the riser and U_t the particle terminal velocity [17].

$$W_b = K\sqrt{h}(U_2 - U_t) \quad (3)$$

The bed height (h) in the gasification reactor depends linearly on the total bed inventory B in the whole facility. This approximation is acceptable in the limit the bed amount in the riser is negligible with respect to B, as confirmed by fluid-dynamic experiments in a

Table 1. Input variables of the model and relevant results

Fuel		Base-case								
Proximate analysis										
Moisture	%	12.0	12.0	12.0	12.0	12.0	12.0	12.0	15.0	20.0
Ash	%	1.0	1.0	1.0	1.0	1.0	1.0	1.0	1.0	0.9
C fixed	%	15.0	15.0	15.0	15.0	15.0	15.0	15.0	14.5	13.6
Volatiles	%	72.0	72.0	72.0	72.0	72.0	72.0	72.0	69.5	65.5
Ultimate analysis (daf)										
C	%	42.0	42.0	42.0	42.0	42.0	42.0	42.0	42.0	42.0
H	%	6.5	6.5	6.5	6.5	6.5	6.5	6.5	6.5	6.5
O	%	51.0	51.0	51.0	51.0	51.0	51.0	51.0	51.0	51.0
N	%	0.5	0.5	0.5	0.5	0.5	0.5	0.5	0.5	0.5
Thermochemistry data										
Heat of pyrolysis	kJ/kg	15500	15500	15500	15500	15500	15500	15500	15500	15500
Heat of pyrolysis	kJ/kg	1533	1533	1533	1533	1533	1533	1533	1533	1533
Volat. formation enthalpy	kJ/mol	−505	−505	−505	−505	−505	−505	−505	−505	−505
Heat transfer coef. wall	$W/m^2/K$	300	300	300	300	300	300	300	300	300
Combustion zone										
Sand size	mm	0.2	0.2	0.2	0.2	0.2	0.2	0.2	0.2	0.2
Cross flow section	m^2	0.0048	0.0048	0.0048	0.0048	0.0048	0.0048	0.0048	0.0048	0.0048
Combustor temperature	°C	743	681	642	767	730	732	722	726	702
Air temperature	°C	25	25	25	25	25	25	25	25	25
Air flow rate	kg/h	12	14	16	12	12	12	12	12	12
Air/fuel ratio		2.4	2.8	3.2	2.4	2.4	2.4	2.4	2.4	2.4
Internal circ. rate	kg/h	279	583	918	250	290	244	213	224	150
Excess air factor	kg/h	1.40	1.63	1.86	1.40	1.40	1.40	1.40	1.45	1.54
Fluidization velocity	m/s	2.03	2.23	2.44	2.08	2.01	2.01	1.99	2.00	1.95
Pyrolysis Gasification zone										
Bed inventory	m^2	20	20	20	10	30	20	20	20	20
Coef. of bed flow rate K'	$kg^{1/2}m^{-1}$	2000	2000	2000	2000	2000	2000	2000	2000	2000
Cross flow section	°C	0.025	0.025	0.025	0.025	0.025	0.025	0.025	0.025	0.025
Reactor temperature	°C	638	620	602	628	644	618	599	613	575
Steam temperature	kg/h	300	300	300	300	300	300	300	300	300
Fuel flow rate	kg/h	5	5	5	5	5	5	5	5	5
Fuel comb. enthalpy	kJ/h	68200	68200	68200	68200	68200	68200	68200	65875	62000
Steam flow rate	kg/h	2	2	2	2	2	3	4	2	2
Steam/fuel ratio	kg/kg	0.4	0.4	0.4	0.4	0.4	0.6	0.8	0.4	0.4
Char flow rate	kg/h	0.80	0.80	0.80	0.80	0.80	0.80	0.80	0.77	0.73
Volatiles flow rate	kg/h	3.60	3.60	3.60	3.60	3.60	3.60	3.60	3.48	3.27
Fluidization velocity	m/s	0.092	0.090	0.088	0.091	0.092	0.134	0.175	0.089	0.085
Syngas										
CH_4		0.007	0.011	0.017	0.009	0.006	0.006	0.005	0.011	0.019
CO		0.079	0.072	0.064	0.075	0.08	1.053	0.036	0.064	0.043
CO_2		0.158	0.162	0.167	0.160	0.156	0.153	0.145	0.161	0.164
H_2		0.392	0.387	0.377	0.390	0.393	0.357	0.326	0.378	0.344
H_2O		0.363	0.36	6.373	0.364	0.362	0.430	0.486	0.384	0.429
N_2		0.002	0.002	0.002	0.002	0.002	0.002	0.001	0.002	0.002
C(gr)		0.000	0.000	0.000	0.000	0.000	0.000	0.000	0.000	0.000
Syngas mol. weight	kg/mol	0.016	0.016	0.016	0.016	0.016	0.016	0.016	0.016	0.017
H_2 yield	kg/kg	0.069	0.068	0.065	0.068	0.069	0.072	0.074	0.069	0.065
Syngas comb. enthalpy	kJ/h	47596	47275	46818	47419	47684	47174	46796	45532	41963
Efficiency		0.70	0.69	0.69	0.70	0.70	0.69	0.69	0.69	0.68

cold ICFB model [13]. Thus, Eq. (3) can be replaced by Eq. (4)

$$W_b = K'\sqrt{B}(U_2 - U_t) \quad (4)$$

Since the temperature T_2 is dependent on the reactor temperature T_1 via Eq. (2), an iterative procedure is required for the solution of the combined system of equations. A trial value of T_1 is assumed in order to calculate T_2 and ΔH, to execute the CEA routine, and to obtain an updated value for T_1. The procedure rapidly converges. The constant K' has been experimentally determined in a scaled cold model of the simulated ICFB gasifier [13].

RESULTS AND DISCUSSION

Table 1 reports the input variables for the model (highlighted in the first column) as well as the most relevant results. The values have been chosen with reference to the geometry of an ICFB gasification facility under construction at JRC/IE (2.5 m high, 80 mm ID for the internal riser and 234 mm ID for the external column). Chipped wood has been assumed as fuel. The excess air ratio has been computed on the basis of fuel char only. Calculations have been repeated by changing one at a time (i) the bed inventory, (ii) the steam/fuel ratio, (iii) the air/fuel ratio, and (iv) the fuel moisture content. These changes are highlighted in the table. The process efficiency (z) has been evaluated as the ratio between the combustion enthalpies of syngas and fuel. An approximately constant value of z (around 0.70) is shown in Table 1, even for changing the operating variables. A slight decrease of the efficiency at higher fuel moisture is predicted due to the increased heat required for drying the fuel.

Fig. 2 shows the composition of the syngas for the base-case set of input variables that is reported in the third column of Table 1. The molar fractions are also reported on H_2O free-basis for comparison. It appears that the CH_4 concentration is very low, because of the relatively high temperature in the gasifier (T_1=638 °C), the endothermic steam reaction $CH_4+H_2O=3H_2+CO$ being favored at high temperature. In fact, the molar fraction of CH_4 at equilibrium decreases from 0.182 to 0.049 when the temperature increases from 561 up to 717 °C, for a 1 : 1 molar CH_4/H_2O system. As far as N_2 concentration is concerned, the ICFB clearly attains a very low, roughly zero concentration, because the biomass is gasified only by steam. This is also reflected in the high value of the H_2 concentration that

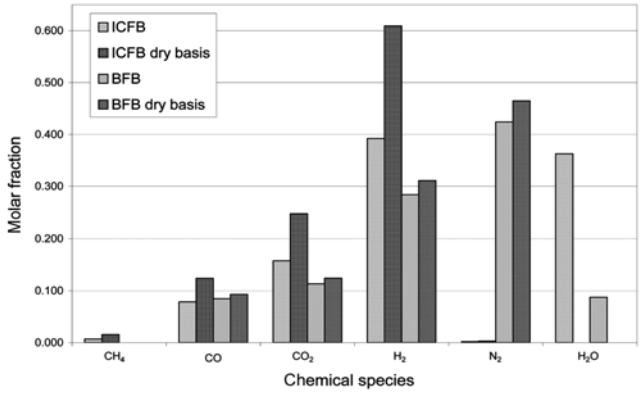

Fig. 2. Major components in the syngas on wet and dry basis (base-case of calculations) and comparison between ICFB and BFB.

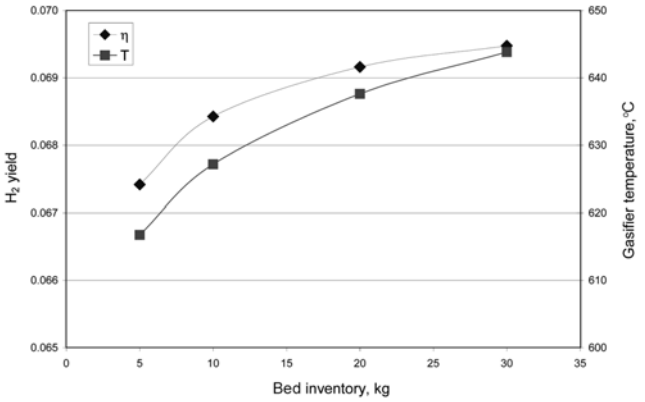

Fig. 3. H_2 yield and gasifier temperature versus the bed inventory.

attains the noticeable value of 0.61 on H_2O free basis. In the same figure, the results of CEA calculations for single stage gasification (bubbling fluidized bed BFB) are also reported for comparison. It clearly appears that the ICFB gasification concept produces higher concentrations of desired species (e.g., H_2).

The dimensionless H_2 yield (η) and the gasifier temperature (T_1) are reported in Fig. 3 as a function of the total bed inventory (B), where h is defined as the mass ratio between the produced hydrogen and the fed fuel. In spite of the large increase of the bed inventory from 5 to 30 kg, the gasifier temperature exhibits a limited increase of around 30 °C, the bed circulation rate and, consequently, the thermal exchange being improved. The temperature difference between combustion and gasification zones also decreases, but not enough to achieve similar values (T_1=644 °C and T_2=730 °C at B= 30 kg), meaning that a very high circulation rate is required for achieving isotherm conditions between the interconnected zones. In turn, η also increases by virtue of the favorable shift in the thermodynamic equilibrium of the gasification reactions at higher temperatures.

Fig. 4 shows the dependence of η and T_1 on the steam/fuel ratio (Ψ). The higher the steam/fuel ratio, the lower the specific enthalpy of reactants entering the gasification stage, the lower is the resulting gasifier temperature. In contrast, the H_2 yield increases with Ψ, since higher H_2O concentration shifts toward the right the equilibrium of the steam reaction $CO+H_2O=CO_2+H_2$. Equilibrium calcu-

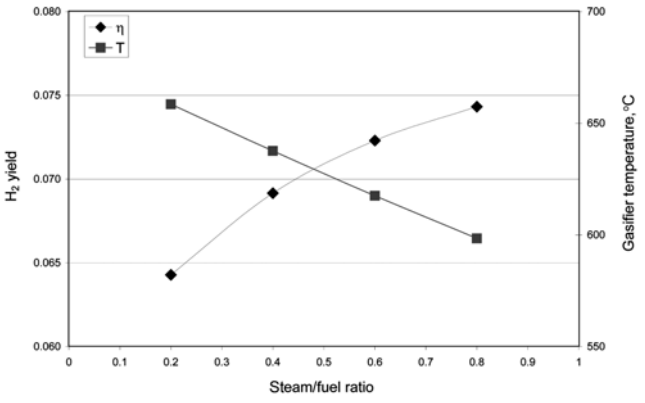

Fig. 4. H_2 yield and gasifier temperature versus the steam/fuel ratio.

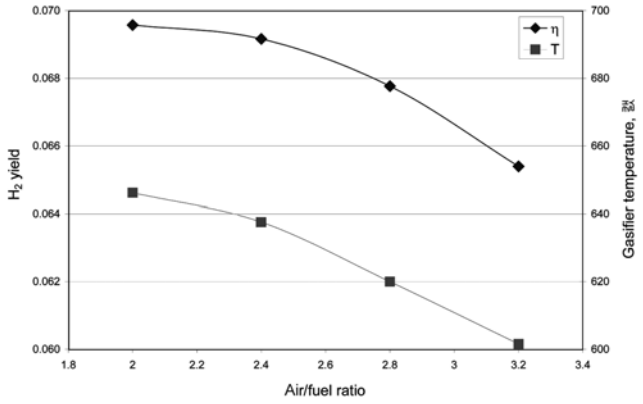

Fig. 5. H_2 yield and gasifier temperature versus the air/fuel ratio.

lations for the steam reaction show that the H_2 molar fraction increases three times when the steam concentration is doubled at fixed CO concentration, for conditions that are similar to those of Fig. 4. At higher values of Ψ, an asymptotic value is achieved for the H_2 molar fraction.

The combined influence of the air/fuel ratio (e) and the fluidization velocity U_2, on η and T_1 is illustrated in Fig. 5. It is worth noting that in this diagram the fuel flow rate is fixed and e varies by changing the air flow rate in the riser. Both variables η and T_1 steadily decrease with e because of the dilution effect in air and the lower temperature attained in the combustion zone. The nonlinear behavior, that is more marked for of T_1, is due to the effect of approaching the slip velocity. As e decreases by moving from the right to the left of the diagram, the increase in the combustor temperature is partly compensated by the lower bed circulation rate, the fluidization velocity U_2 decreasing and approaching the limit value U_t= 1.85 m/s, for a sand size of 2.0 mm.

The dependence of η and T_1 on the fuel moisture content (f) is shown in Fig. 6. It appears that higher moisture content exerts a detrimental effect on both gasifier temperature and H_2 yield. In particular, T_1 linearly decreases with f, a larger energy being required for the vaporization stage in the gasifier. Nevertheless, higher f leads to an increased steam concentration upon evaporation that slightly

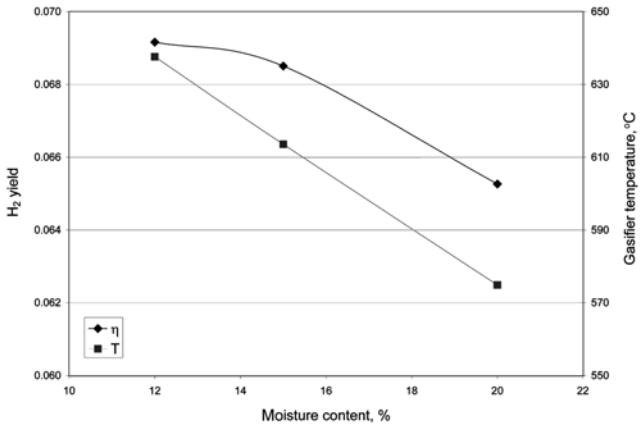

Fig. 6. H_2 yield and gasifier temperature versus the fuel moisture content.

compensates the energy loss effect on the H_2 yield, as shown on the left side of the diagram.

Losses in efficiency could arise from mutual leakages in the two interconnections between the combustor and the gasifier. In the bottom section, gas from the gasifier enters the combustor together with bed materials. Similarly, in the top section exhausts can pass to the gasification vessel and, consequently, dilute/burn the syngas. In particular, the bottom leakage from the gasifier to the combustor is unavoidable, the gas being entrained together with the solid flow, and plays a larger role with respect to the top leakage. Some calculations have been performed assuming that a fraction ξ of the steam leaks from the gasifier to the combustor. Both combustor and gasifier temperatures decrease at increasing leakage: for base case conditions, T_2 decreases from 743 to 714 °C as ξ increases from 0.0 to 0.2. In turn, an effect on syngas composition is exerted because of the lower gasifier temperature and the different mixing between the reactants. The higher ξ, the lower H_2 concentration and the higher CH_4 concentration. However, a slight effect is noted on the whole gasification efficiency.

CONCLUSIONS

The application of a thermodynamic model to a simplified scheme of ICFB gasifier allowed the estimation of the syngas temperature and its composition. The model predicts H_2 concentration up to 61% on water free basis. The comparison between one-stage gasification and the internal circulating fluidized bed scheme is notably favorable for the ICFB process.

The dependence of the most important model results on a set of operating conditions has been evaluated. Among these the bed inventory, the steam/fuel ratio, the air/fuel ratio, and the moisture content in the fuel have been varied over a realistic range. The largest changes for the hydrogen yield have been noted by changing the steam/fuel ratio as well as the fuel moisture, since these variables affect both the equilibrium temperature and H_2O concentration.

Nevertheless, in a real system the achievement of thermodynamic equilibrium is unlikely, particularly for the steam reforming reaction of methane. Thus, the model estimates of H_2 concentration and yield must be considered as optimistic and as a theoretical upper limit.

Losses in efficiency due to the mutual leakages in the interconnections between the combustor and the gasifier can have detrimental effects on the temperature of combustion and gasification zones, as highlighted by model calculations. The extent of leakage (10-30%) strongly depends on the design of the gasifier as well as on the operating conditions. The mechanism and minimization of the leakage deserve further study, also in the modeling activity.

ACKNOWLEDGMENT

Bonnie J. McBride and Sanford Gordon of NASA are gratefully acknowledged for the CEA software they have freely distributed. The work was carried out, in part, within the European Commission's research and development program.

NOMENCLATURE

B : total bed inventory [kg]

e : air/fuel ratio [kg/kg]
f : fuel moisture content [%]
K : coefficient for bed flow rate [kg $m^{-1.5}$]
K′ : coefficient for bed flow rate [$kg^{0.5}$ m^{-1}]
h : bed height [m]
S : surface of heat transfer [m^2]
T : temperature [K]
U : fluidization velocity [m/s]
U_t : terminal velocity [m/s]
W : mass flow [kg/s]
z : process efficiency [-]

Greek Letters

γ : specific heat [J/(kg K)]
ΔH : heat transfer rate [W]
η : H_2 yield [kg/kg]
Θ : heating value [J/kg]
Λ : coefficient of heat transfer [W/(m^2 K)]
ξ : leakage fraction [kg/kg]
Ψ : steam/fuel ratio [kg/kg]

Subscripts

a : air
b : bed
ch : char
ex : exhausts
ref : reference conditions
1 : bubbling FB gasifier
2 : combustor (riser)

REFERENCES

1. European Commission, *Green paper. Towards a european strategy for the security of energy supply*, Office for Official Publications of the European Communities L-2985 Luxembourg, ISBN 92-894-0319-5 (2001).
2. A. V. Bridgewater, *Fuel*, **74**, 631 (1995).
3. K. V. Lobachov and H. J. Richter, *Energy Convers. Mgmt.*, **39**, 1931 (1998).
4. U. Arena and A. Cammarota, *Proceedings of 14th FBC Conference*, Vancouver, 433 (1997).
5. F. Miccio, O. Moersch, H. Spliethoff and K. R. G. Hein, *Proceedings of 15th FBC Conference*, Savannah, 108 (1999).
6. M. K. Ko, W. Y. Lee, S. B. Kim, K. W. Lee and H. S. Chun, *Korean J. Chem. Eng.*, **18**, 961 (2001).
7. L. Devi, K. J. Ptasinski and F. J. J. G. Janssen, *Biomass & Bioenergy*, **24**, 125 (2003).
8. R. Chirone, L. Massimilla and P. Salatino, *Prog. Energy Combust. Sci.*, **17**, 297 (1991).
9. F. Miccio, O. Moersch, H. Spliethoff and K. R. G. Hein, *Fuel*, **78**, 1473 (1999).
10. H. Hofbauer, G. Veronik, T. Fleck, R. Rauch, H. Mackinger and E. Fercher, *Proceedings of developments in thermochemical biomass conversion*, Banff, **2**, 1016 (1997).
11. H. Hofbauer, *Proceedings of 19th FBC Conference*, Vienna, CD, invited lecture (2006).
12. F. Miccio, *Korean J. Chem. Eng.*, **21**, 404 (2004).
13. F. Miccio, K. Svoboda, J. P. Schosger and D. Baxter, *Proceedings of 19th FBC Conference*, Vienna, CD, paper 58, (2006).
14. S. Gordon and B. J. McBride, *NASA report*, ref. pub. 1311 (1994).
15. N. M. Laurendeau, *Prog. Energy Combust. Sci.*, **4**, 221 (1978).
16. D. E. Daugaard and R. C. Brown, *Energy & Fuels*, **17**, 934 (2003).
17. D. Kunii and O. Levenspiel, *Fluidization engineering*, Butterworth-Heinemann, Boston, 61 (1991).